Numerical analysis of natural convection of ferric oxide-water nanofluid flow in a wavy staggered cavity energized by a chemical exothermic reaction

Farooq H. Ali*[1], Hussein H. Alaydamee[2], Qusay H. Al-Salami[3], Hameed K. Hamzah[4], Mohammed Azeez Alomari [5,6], Qusay Rasheed Al-amir[7]

[1] Mechanical Engineering Department, College of Engineering, University of Babylon, Babylon, Iraq

Email: eng.farooq.hassan@uobabylon.edu.iq

[2] Department of Chemical Engineering, University of Al-Qadisiyah, College of Engineering, Al-Qadisiyah, 58002, Iraq

Email: Hussein.hantoosh@qu.edu.iq

[3] Department of Business Administration, College of Administrative and Financial Sciences, Cihan University-Erbil, Iraq
Email: qusay.hameed@cihanuniversity.edu.iq

[4] Mechanical Engineering Department, College of Engineering, Babylon University, Babylon, Iraq

Email: eng.hameed.hamzah1@uobabylon.edu.iq

[5] Department of Mechanical Engineering, University of Al-Qadisiyah, Al-Diwaniyah, 58001, Iraq

[6] College of Engineering, University of Warith Al-Anbiyaa, Karbala, Iraq

Email: mohammed.hasan@qu.edu.iq

ORCID:https://orcid.org/0000-0002-3223-9476

[7] Air Conditioning and Refrigeration Techniques Engineering Department, Al-Mustaqbal University, Babylon 51001, Iraq

Email: Qusay.Rasheed.AbdAl-amir@uomus.edu.iq

Abstract

Over the last 28 years, numerous investigations have been conducted to enhance common fluids, **such as** ferric oxide-water nanofluid. In this study, we examine the time-dependent natural convection of such nanofluid under the influence of exothermic reactions, utilizing Finite Element Method. The key governing parameters considered include Ra (10^3-10^5), Ha (0-60), F_k (0-4), enclosure wavelength (0-3 waves), magnetic field inclination angle ($0°$-$90°$), and nanoparticle volume fraction (0-0.08). Our findings show that the mean Nusselt number (Nu) increases by 142.85% for Ha=12, Φ =0.02, and F_k=1 at 5 seconds when Ra is increased to 10^5 in conjunction with double-wave active walls. Furthermore, when there is no magnetic field, increasing F_k from 0 to 4 results in a 76.12% rise in Nu_{avg} for Ra=10^5 and Φ =0.04. When the volume percentage of nanoparticles is increased from 0 to 0.08, the heat transmission increases by 16.34% for Ra=10^5 and F_k=1. This study reveals complex relationships between operating parameters and offers insightful views for the development of systems including exothermic reactions, thermal behavior, and nanofluid dynamics. This work offers recommendations for enhancing thermal systems incorporating nanofluids by shedding light on the intricate interactions between exothermic processes, magnetic fields, and nanoparticle dynamics.

Keywords: *natural convection, exothermic reaction, Ferric oxide, nanofluid, Staggered enclosure, numerical analysis, MHD*

present address: [7]Mechanical Power Engineering Department, College of Engineering and Technologies, Al-Mustaqbal University, 51001, Babylon, Iraq

Nomenclature

a	Reactant concentration in [mol.m^{-3}]	**Subscripts**	
B_o	Magnetic field impact in [Ωkg m^{-1} s$^{-0.5}$]	h	High-temperature field
c_p	Specific heat [J Kg^{-1} K^{-1}]	c	Low-temperature field
E	Activation energy in [J.mol^{-1}]	b	Base fluid
F_k	Chemical reaction parameter (Frank_Kamenetskii)	nf	Nanofluid
g	Gravitational force [m s^{-2}]	p	Solid particle
Ha	Hartmann-number (dimensionless)	**Greek Symbols**	
k_o	Pre-exponential factor in [s^{-1}]	τ	Time (dimensionless)
L	Dimensionless length of cavity	γ	Angle
MHD	Magnetohydrodynamics	ρ	Density [$kg\ m^{-3}$]
Nu_L	Local Nusselt number (dimensionless)	k	Thermal, conductivity of fluid [$W\ m^{-1}K^{-1}$] or [$J\ m^{-1}\ K^{-1}\ s^{-1}$]
Nu_{ave}	Average Nusselt number (dimensionless)	ϕ	Volume fraction of nanoparticles
Nu	Nusselt number (dimensionless)	σ	Electrical conductivity [$S\ m^{-1}$]
P	Pressure term (dimensionless)	α	Diffusivity parameter (thermal) [m^2s^{-1}]
p	Pressure in [kg m^{-1} s^{-2}] (dimensional parameter)	v	Kinematic viscosity in [m^2 s^{-1}]
$\Pr$	Prandtl number (dimensionless)	β	Thermal expansion coefficient in [K^{-1}]
q	Heat flux	σ^*	Stefan-Boltzmann constant
q_r	Heat flux (radiative) in [kg s^{-1}]	$\rho\beta^{/}$	Volumetric expansion of mass
Q	Reaction exothermicity in [J mol^{-1}]	$\rho\beta$	Volumetric expansion of thermal
R	Fluid constant in [J k^{-1} mol^{-1}]	θ	Temperature (dimensionless)
Ra	Rayleigh number (dimensionless)	μ	Dynamic viscosity in [$kg\ m^{-1}\ s^{-1}$]
R_V	Magnitude of velocity (dimensionless)	ρc_p	Heat capacitance in [$J\ m^{-3}\ K^{-1}$]
r	Reaction rate in [kmol m^{-3} s^{-1}]		
T_o	Constant temperature in [K]	λ	Fluid conductivity in [$W\ m^{-1}\ K^{-1}$]
T	Fluid temperature in [K]	Ψ	Stream function
T_h	Hot wall temperature in [K]	Ω	Vorticity
T_c	Cold wall temperature in [K]	ξ	Dimensionless vorticity
U	Component of velocity in x direction (dimensionless)	ε	Surface emissivity
V	Component of velocity in y direction (dimensionless)		
u	Component of velocity in x direction in [m/s]		
v	Component of velocity in y direction in [m/s]		
X,Y	Cartesian coordinates (dimensionless)		
x, y	Cartesian coordinates in [m]		

1. Introduction

Nowadays, researchers' efforts are undergoing a rapid analysis of heat transfer efficiency due to its widespread influence in many engineering fields [1]. The majority of these efforts were focused on enhancing the heat transfer rate by creating diverse heat transfer materials and mediums to augment the efficiency of heat transfer [2]–[7]. Numerous experiments and mathematical analyses have been conducted on convective heat transfer and the flow of nanofluids in enclosed spaces due to their broad applications in chemical reactors, electronic cooling devices, heat exchangers, solar generators, etc. [8]–[11]. As chemical processes continue to evolve and demand heightened control and optimization, understanding the dynamic relationship between fluid movement driven by buoyancy forces and the heat generated by exothermic reactions becomes imperative [12]–[14]. For instance, natural convection in batch or catalytic reactors contributes to temperature control by facilitating the movement of the reacting fluid, ensuring uniform temperature distribution, and preventing localized overheating in the presence of exothermic reactions [15]–[18].

1.1. Natural convection in cavities

Investigation of natural convection in closed enclosures is a necessary study for many scientists due to its wide range of applications in engineering[19], [20]. Izadi et al. [21] made a comparative review of heat transfer studies of nanofluids in many shapes of cavities including square cavities. They concluded that the majority of the studies have documented a significant improvement in heat transfer as the volume concentration of nanoparticles, Reynolds number, and Richardson number increase. Wang et al. [22] have looked at the numerical studies of the nanofluids free convection within a partially heated square enclosure utilizing Buongiorno's model. The influence of Ra, nanoparticles diameter, walls temperature gradient, heater position and length, and nanoparticles distribution were investigated and noted that at low Ra numbers, there is a rising trend in heat transfer rate with an increase in nanoparticle volume fraction. Conversely, at high Ra numbers, the heat transfer rate reaches its peak. Additionally, as the length of the heater increases, both the average Nu and heat transfer enhancement experience a decline. Uddin et al. [23] conducted a numerical investigation of the heat transfer performance in a wavy vertical walls square enclosure including CuO-H_2O nanofluid flow with a hydro-magnetic field. Their results showed that for a nanofluid with a lower nanoparticle volume fraction, there was an elevation in the range of velocity, streamline effectiveness, isotherms efficacy, and uniformity of isoconcentration labeling with an increase in the thermal Ra number. In the vertical magnetic field, effective flow happens as the magnetic pitch gets stronger and the flow intensity drops. When more waves occur on a vertical surface, flow complexity

increases. When the Ra value rises from 104 to 106, the average heat transmission increases by 158%. An increase of 10.18% is observed in the mean heat transfer when the nanoparticle volume fraction is increased from 0.025 to 0.05. On the vessel's non-wave vertical surface, there is a higher rate of heat transfer. Heat transmission increases by 3.62% when the wave number is raised from 2 to 4 and drops by 16.98% when the wave number is raised to 2. Rashid et al. [24] analyzed the influence of nanoparticles on the nanofluid flow and heat transfer within a square enclosure containing a fixed circular object. Their work explained how the form of the nanoparticles affects the flow of the nanofluid in a lid-driven square cavity that has a stationary-centered circular obstruction. According to their results, non-spherical shape nanoparticles performed better in heat transfer and temperature distribution than diamond-water nanoparticles. Saha et al. [25] examined the MHD natural convection flow behavior in the presence of a heated fin within a wavy square cavity using nanofluids.   The result showed that the temperature flow varies dramatically as all of Ra number, Ha number, and nanoparticle volume increase in value. The volume of the nanoparticles, Ra number, and Ha number have a substantial impact on the average Nu number. It is also noted that streamlines and isotherms alter in tandem with fin length variations. Furthermore, for blade-shaped nanoparticles, the temperature transmission rate increased by 7.65%, whereas for spherical-shaped nanoparticles, it increased by 2.86%. In Boukendil et al. [26] research, two square isothermal cylinders kept at different temperatures inside a square enclosure and were numerically tested for examining laminar natural convective heat flow and surface radiation. Their findings demonstrated that, particularly at high Ra numbers, surface radiation has a significant impact on the annulus flow structure. They discovered that both convective and radiative heat transfers are significantly influenced by the sizes, sides-ratio, and placements of the inner square cylinders.

1.2. Natural convection of nanofluid in cavities

Nanoscale particles of less than 100 nm in diameter or fibers suspended in a base fluid are known as nanofluids [27]. These liquids are better when spreading and dispersing because of their improved viscosity. Recently, hybrid nanofluids have been utilized by many scientists [28], [29] and have shown great promise in heat transfer enhancement [30] which can be seen in Ashorynejad and Shahriari's findings, that, the effect of the presence of nanoparticles concerning Ra number caused the magnetic field to grow or fall. Ra = 10^5 has a favorable contribution from the increasing phase deviation. Mansour et al. [31] studied the impact of heat source on natural convection when utilizing a hybrid nanofluid equipped in a square porous cavity that was differentially heated and cooled by a heat source. Their study concentrated on analyzing the natural

convection flow, entropy production, and magnetohydrodynamics of heat transfer in the presence of water and Al_2O_3 and found that when compared to other nanoparticles, Cu can be added to achieve the maximum heat transfer rate. Sheikholeslami et al. [32] discussed the influence of CuO-water nanofluid MHD natural convection in a porous media cavity of complex shape applying thermal radiation. It tested the impact of different parameters including Ha number, radiation parameter, volume fraction of nanofluid, Ra number etc. They came up with the conclusion that heat transfer saw a good enhancement when augmenting Ra and Darcy members. The same nanofluid was investigated by Rashad et al. [33] research which numerically examined the influences of heat source inside an inclined square enclosure of porous media on MHD natural convection in the presence of entropy generation. Their outcomes stated that diminishing convective heat transfer was caused by the rise of nanoparticle volume fraction. Sajjadi et al. [34] utilized the Cu/water nanofluid in their study of MHD natural convection in three-dimensional cavity. They studied the impact of different parameters including Ra number, Ha number, and nanoparticle volume fraction. Their results indicated that as the Ha number rises, convection heat transfer diminishes. The average Nu number also falls for the vertical walls, although it reduces more for the right than for the left. The average Nu number decreases by 64% for the left wall and 70% for the right wall as the Ha number increases from 0 to 50. Kodi et al. [35] have looked at the flow of MHD mixed convection and maxwell nanofluid utilizing a porous vertical cone with variable heat conductivity. Their findings stated that reduced velocity was the result of increased Maxwell and magnetic parameters. While the temperature increased with increasing radiation and thermophoresis parameters, the Prandtl number and Brownian motion parameters saw a decrease. In Al-Amir et al. [30] work, which focused on analyzing natural convection utilizing TiO_2-water nanofluid inside a z-staggered cavity of porous media, indicated that the highest streamline values decrease as the nanofluid's density rises. Mourad et al. [36] equipped a hybrid nanofluid (Fe3O4-MWCNT/Water) inside a porous cylindrical cavity containing a Koch snowflake to study the MHD natural convection. Their study included the influence of the volume fraction of nanoparticles, Ha number, Ra number, Darcy number, etc. Solid nanoparticles enhanced thermal conductivity, which enhanced heat transfer, as would be expected. Heat transfer between the hot and cold sources was sped up by raising the Ra number and boosting the flow rate in the cavity. Different heat source objects were introduced by Tasnim et al. [37] research to research the MHD natural convection of square cavity occupied by TiO_2-water nanofluid. Observations have been made regarding the impact of the Ha number, Joule heating parameters, nanoparticle volume fraction, cavity inclined angle, and various locations of heat source objects. The investigation demonstrated that when the volume fraction of nanoparticles decreases, convective heat transfer increases. Geridonmez and Oztop [38] researched natural convection in an enclosure using Al_2O_3/Water nanofluid with a partial magnetic field. They have concluded that when intensifying nanoparticles, extending the length of the

partial heater, and raising the Ra number, convective heat transfer increases while it decreases when the Lorentz force increases.

1.3. *Exothermic reactions*

Engineering applications such as chemical separation, oil separation, and combustion reactions which involve heat transfer in the presence of nanofluids chemical reactions are affected significantly by exothermic chemical reactions. Investigating this phenomenon is becoming essential to many innovators and researchers [39]–[42] due to its universal prevalence in many industries, such as the electronic cooling industry, power industry, and chemical industry. For example, in a nuclear power plant, maintaining safe operating temperatures for the nuclear reactor is necessary. When chemical reactions occur within the reactor coolant loop, enhancing the heat transfer characteristics of nanofluids can improve the efficiency of heat removal from the reactor core. Producing chemicals or fuels is another example where catalytic reactions occur in various processes resulting in heat generation which can be controlled by nanofluids. Employing nanofluids in the heat exchanger of chemical reactors can enhance heat transfer during catalytic reactions. This enhancement of heat transfer with nanofluids improves the overall efficiency of catalytic reactions, leading to higher yields and reduced energy consumption [43]. Arifuzzaman and Uddin [44] studied the natural convection of nanofluid in a square object under the existence of exothermic reaction and magnetic field. They have concluded that raising Ra number from 10^5 to 10^6 resulted in an enhancement of the heat transfer by almost 72.78%. It is also noted from their results that aluminum/water nanofluid flow and heat transfer are regulated by the magnetic field and the Arrhenius chemical reaction parameters. In Rahman et. al. [45] numerical analysis, a porous cavity, equipped with nanofluid, was investigated to study the natural convection flow under the application of variable angle magnetic field and exothermic reaction. They noticed that adjusting the enclosure's inclination counterclockwise increases the Frank-Kamenetskii number and regulates the rate of heat transfer. In addition, the results stated that a high Frank-Kamenetskii number causes the magnetic field slope to outweigh the rate of heat transfer. Yadav [46] demonstrated the effects of a chemical reaction on heat transfer utilizing three different types of porous cavities, square, rectangular, and slender, equipped with different types of nanofluids, Ag/water, Cu/water, Al_2O_2/water, and TiO_2/water. The findings showed that increasing the modified Lewis, the Ra-Darcy number of the nanoparticle, and the chemical reaction parameter causes convection to commence quickly. In contrast, the heat capacity ratio has no effect on the beginning of convection, hence increasing the pace of heat transfer within porous cavities. Raising the thermal conductivity ratios and heat capacity increases the quantity of heat transmission. When it comes to rectangular enclosures, the heat transmission decreases with the aspect

ratio; however, this phenomenon is not observed in slender or square enclosures. Furthermore, in comparison to the base fluid of water, the heat transfer intensified by 22.7%, 20.8%, 19.8%, and 18.9% for the Water-Al2O2, Water-TiO2, Water-Cu, and Water-Ag nanofluids, respectively. Other Recent articles primarily focus on studying the stability, convective behavior, and thermal dynamics of Casson nanofluids or Jeffrey fluids within porous or permeable layers, examining effects from factors like rotation, viscosity changes, throughflow, viscous dissipation, chemical reactions, and magnetic fields on nanofluid convection and instability in various confined environments[47]–[49].

Our knowledge of natural convection phenomena is greatly advanced by this computational study, which focuses on the FeO_4-H_2O nanofluid in a complicated geometry with two circular objects under the effect of an exothermic reaction. By using the finite element method to solve the related partial differential equations, this study not only addresses a very specific issue but also closes a large knowledge gap. Recent research shows that there aren't many studies on this particular problem, which highlights the study's originality and makes it crucial for theoretical development as well as possible real-world applications.

2. Physical Model, Mesh Dependency, and Validation

This study considers a complicated cavity with two circular, equilateral barriers. The staggered enclosure's right and left vertical wavy walls are at high temperatures while the middle non-wavy ones are at low temperatures. All horizontal walls of the complex cavity and the circular obstacles are isolated. A magnetic field, natural convection, and nanofluid flow have been judged inside the cavity. Figure 1 illustrates the complicated enclosure with the physical description. The lower-left corner of the cavity represents the origin of the coordinate. The horizontal and vertical walls are represented by the x-axis and y-axis respectively. Fe_3O_4/water nanofluid thermophysical properties in Table 1 are applied in the simulation. Because the postulated problem's solutions are straightforward, the radiation influence is disregarded in this study's application of Arrhenius chemical processes connected to the presence of a magnetic field. Utilizing the hydromagnetic field and its inclination angle, the momentum equations are integrated to comprehend heat transfer and flow dynamics when a magnetic field is present.

As illustrated in Table 2, the number of elements used for the mesh of the current problem is 21622 when comparing the Nusselt number for a fixed value of Ra=10^4, Ha=14, F_k=2, Φ =0.03, and time=5 sec.

Figure 2 shows the validated comparison of the current analysis to a previously published paper (Mehedi et. al [43]), the comparison was made under the assumption of constant values of $\Phi = 0.05$, $Ha = 40$, $F_k =$

2, $\gamma = 0$, Ra=10^4, $T_0 = 25$ and τ=5 sec, in terms of streamlines and isothermal contours. As illustrated by the validation figures, the present coding comes to high agreement with the published coding of the problem discussed by the author.

3. Modeling

This study model takes into account the 2D unsteady laminar natural convection of iron oxide/water nanofluid, identifying nanosolids as the main fluid species, to evaluate the heat transfer and fluid flow behavior in wavy complicated cavities. The Arrhenius equation, which states that the first-order chemical reaction rate is constant and dependent on the absolute temperature, is used to study the exothermic chemical processes occurring in geometry. Lazarovici et al. [50] states that it may be represented as follows:

$$r = k_0 a e^{(-\frac{E}{RT})} \tag{1}$$

To solve the above problem, the following equations are considered [51], [52]:

$$\frac{\partial u}{\partial x} + \frac{\partial v}{\partial y} \tag{2}$$

$$\frac{\partial u}{\partial t} + \left(u\frac{\partial u}{\partial x} + v\frac{\partial u}{\partial y} \right) = -\frac{1}{\rho_{nf}}\frac{\partial p}{\partial x} + v_{nf}\left(\frac{\partial^2 u}{\partial x^2} + \frac{\partial^2 u}{\partial y^2} \right) + \frac{\sigma_{nf}B_o^2}{\rho_{nf}}.\sin(\gamma)\left[v.\cos(\gamma) - u.\sin(\gamma) \right] \tag{3}$$

$$\frac{\partial v}{\partial t} + \left(u\frac{\partial v}{\partial x} + v\frac{\partial v}{\partial y} \right) = -\frac{1}{\rho_{nf}}\frac{\partial p}{\partial y} + v_{nf}\left(\frac{\partial^2 v}{\partial x^2} + \frac{\partial^2 v}{\partial y^2} \right) + g\beta_{nf}\left(T - T_c \right) + \frac{\sigma_{nf}B_o^2}{\rho_{nf}}.\cos(\gamma).\left[u.\sin(\gamma) - v.\cos(\gamma) \right] \tag{4}$$

$$\frac{\partial T}{\partial t} + u\frac{\partial T}{\partial x} + v\frac{\partial T}{\partial y} = \alpha_{nf}\left(\frac{\partial^2 T}{\partial x^2} + \frac{\partial^2 T}{\partial y^2} \right) + \frac{Qm_o}{\rho c_p}ce^{-\frac{E}{RT}} \tag{5}$$

The unitless parameters are evaluates as:

$$Y = \frac{y}{L}, X = \frac{x}{L}, U = \frac{uL}{\alpha_b}, V = \frac{vL}{\alpha_b}, \tau = \frac{t\alpha_b}{L^2}, P = \frac{pL^2}{\alpha_b^2\rho_b}, F_k = \left(\frac{E}{RT_o} \right)\frac{L^2 Q k_o a}{T_o k_b}e^{-\frac{E}{RT_o}}, Ra = \frac{L^3 g\beta_b RT_o^2}{E\alpha_b v_b}, \Pr = \frac{v_b}{\alpha_b} \tag{6}$$

Therefore, the dimensionless continuity, momentum and energy equations becomes as follows:

$$\frac{\partial U}{\partial X} + \frac{\partial V}{\partial Y} = 0 \tag{7}$$

$$\frac{\partial U}{\partial \tau} + U\frac{\partial U}{\partial X} + V\frac{\partial U}{\partial Y} = -\frac{\partial P}{\partial X} + \frac{\mu_{nf}}{\rho_{nf}\alpha_b}\Pr\left(\frac{\partial^2 U}{\partial X^2} + \frac{\partial^2 U}{\partial Y^2}\right) + Ha^2\Pr.\sin(\gamma)\left[V.\cos(\gamma) - U.\sin(\gamma)\right]$$

(8)

$$\frac{\partial V}{\partial \tau} + U\frac{\partial V}{\partial X} + V\frac{\partial V}{\partial Y} = -\frac{\partial P}{\partial Y} + \frac{\mu_{nf}}{\rho_{nf}\alpha_b}\Pr\left(\frac{\partial^2 V}{\partial X^2} + \frac{\partial^2 V}{\partial Y^2}\right) + \left(\frac{\rho_{nf}\beta_{nf}}{\rho_{nf}\beta_b}\right)\theta.\Pr.Ra + Ha^2\Pr.\cos(\gamma).\left[U.\sin(\gamma) - V.\cos(\gamma)\right]$$ (9)

$$\frac{\partial \theta}{\partial \tau} + U\frac{\partial \theta}{\partial X} + V\frac{\partial \theta}{\partial Y} = \frac{\alpha_{nf}}{\alpha_b}\left(\frac{\partial^2 \theta}{\partial X^2} + \frac{\partial^2 \theta}{\partial Y^2}\right) + \frac{(\rho_b c_{p_b})}{(\rho_{nf}c_{p_{nf}})}F_k e^\theta$$

(10)

The following formulas are insured to evaluate the volumetric thermal and heat capacities, the coefficient of mass expansion, thermal diffusivity, , and effective density of nanofluids [53]:

$$\rho_{nf} = \phi\rho_p + \rho_b - \rho_b\phi$$ (11)

$$\rho_{nf}c_{p_{nf}} = \phi\rho_p c_{p_p} + \rho_b c_{p_b} - \phi\rho_b c_{p_b}$$ (12)

$$\alpha_{nf} = \frac{k_{nf}}{\rho_{nf}c_{p_f}}$$ (13)

$$\rho_{nf}\beta_{nf} = \phi\rho_p\beta_p + \rho_b\beta_b(1-\phi)$$ (14)

Based on Brinkman model, the aluminum oxide/water effective dynamic viscosity is assessed as illustrated in equation (15):

$$\frac{\mu_{nf}}{\mu_b} = \left(\frac{1}{1-\phi}\right)^{2.5}$$ (15)

Thermal conductivity is evaluated base on Bruggeman et al. [54] as shown in equation (16):

$$\frac{k_{nf}}{k_b} = \frac{k_p + 2k_b - 2\phi(k_b - k_p)}{k_p + 2k_b + \phi(k_b - k_p)}$$ (16)

The boundary conditions are expressed as:
At the hot surface:

$$\theta = 1, U = V = 0$$

At the cold surface:

$$\theta = 0, U = V = 0$$

Local and average Nusselt number are determined on the lower straight wall.

$$Nu_L = -\frac{\partial \theta}{\partial X}\frac{k_{nf}}{k_b}$$ (17)

Local and average Nusselt number are determined on the lower straight wall.

9

$$Nu_{ave} = -\frac{1}{0.65} \int_0^{0.65} \frac{k_{nf}}{k_b} \frac{\partial \theta}{\partial X} dY \tag{18}$$

The stream function (Ψ) is written as follows:

$$U = \frac{\partial \Psi}{\partial Y}, V = -\frac{\partial \Psi}{\partial X} \tag{19}$$

4. Results and Discussions

The present work aims to numerically investigate the heat transmission rate of ferric oxide/water nanofluid in a staggered enclosure having double wavy walls on the vertical sides in the presence of a magnetic field and exothermic reaction. The influence of having two circular objects within the complex cavity was also studied. Several governing parameters were studied including the range of Ra number (10^3 to 10^5), Ha number (0 to 60), F_k number (0 to 4), and the volume percent of nanoparticles (0 to 0.08). Based on the provided boundary conditions, the results are presented in terms of isothermal contours and streamlines, and the study included time dependency impacts for different problem parameters.

Figure 3 illustrates the streamlines and isothermal contours for various values of Ra number $10^3 \leq Ra \leq 10^5$ inside the cavity keeping other operating parameters constant (Ha=12, case 2 of two waves, $\Phi = 0.02$, and F_k=1). At low Ra numbers, results note that the nanofluid moves smoothly within the cavity around the circular objects. It is noticeable that the streams in the upper part of the cavity move counterclockwise due to the effect of the high-temperature wavy right wall which drives the streams in that direction. The opposite occurs at the lower part of the cavity since the hot surface is located on the vertical left wall and affects the movement of the nanofluid resulting in a clockwise motion reaching a maximum stream value of 1.8. Augmenting the Ra value to 10^4 results in increasing the fluid flow movement reaching a higher value of 14 and generating a small vortex close to the upper cylinder of the upper part of the cavity. The reason behind this scheme is the rise of buoyancy force strength. As the Rayleigh number (Ra) increases, buoyancy-driven forces create natural convection, which makes the nanofluid circulate more vigorously since they are stronger than viscous forces. The maximum streams even increase to 70 when further amplification of the Ra value of 10^5 results in generating double vortices owing to the rise of buoyancy force strength to the maximum value. One vortex is close to the upper left side of the upper cylinder while the other vortex is positioned close to the upper right side of the lower cylinder due to the direction of stream flow. Isothermal contours at low Ra seem to have a nearly uniform distribution near the active walls showing no high mixing due to the low flow regime. As the buoyancy force becomes higher, Ra= 10^4, the hot fluid tends to distribute around the circular object moving toward the top left direction (counterclockwise direction) at the upper part of the enclosure. The hot wavy surface in the lower part of the cavity pushes the distribution of heat in a clockwise direction toward the top

right part around the circular geometry. Comparing the cold wall to the hot wall, an opposite trend occurred here where the isotherms tend to move downward having more distribution at the bottom of the enclosure. The increase in Ra to 10^5 enhances the heat transmission around the circular objects providing a wide distribution of isotherms at the top section. Increased temperature gradients and more violent fluid motion are caused by higher Ra values, which raise the convective heat transfer coefficient and, in turn, enhance heat transmission. This trend can be confirmed by the data given in Figure 4 which shows the average Nusselt number for the variation of Ra. In comparison, the impact of intensifying Ra value to 10^5 was found to have the optimum rise in Nu_{avg} by 142.85%, while the amplification of Ra to 10^4 saw a slight increase of Nu_{avg} by nearly a 20%. The obtained results come in agreement with the results obtained in recently published work [55].

Figure 5 shows the magnetohydrodynamic impact on the nanofluid streams and heat transfer behavior, utilizing a wide range of Ha values (Ha=0 to 60). At the same time, other parameters are kept at a fixed value (Ra=10^5, $\phi =$ 0.03, F_k=1, and the number of waves= 3). The results indicate that applying a magnetic field has an obvious impact on the flow of the nanofluid that is when there is no magnetic field in the cavity, the streams reach a maximum velocity of 70, but increasing Ha to 12, 25, and 60 causes the maximum streams value to decrease by 14.28%, 28.57%, and 71.43% respectively. The reason for this phenomenon is that the magnetic field creates a Lorentz force that prevents the electrically conducting nanofluid from moving. This resistive force gets greater as Ha rises, slowing down fluid movement and hindering convective currents. On the other hand, augmentation of Hartmann number causes the isothermal lines to have a denser travel downward indicating more heat transmission distribution toward the circular objects. However, it is also noticeable that decreasing Ha leads to enhancing the horizontal heat transfer in terms of isolines in the top part of each circle geometry. The latter trend agrees with the mean Nusselt values shown in Figure 6 which presents the Nu_{avg} values for various Ha ranges, which also satify the same results obtained by the most recently published article [56]. It is shown that diminishing the Hartman number from 60 to 12 leads to a better increase in the mean Nu 3.5 to 7. Additionally, Nu_{avg} was found to increase more effectively reaching 7.6 in the absence of magnetic field.

Figure 7 demonstrates the effects of an exothermic reaction, by variation of Frank-Kamenetskii number $0 \leq F_k \leq 4$, on the heat transmission and stream velocity of ferric oxide/water nanofluid ($\varphi = 0.04$) within the cavity in the absence of magnetic field and keeping Ra=10^5 constant throughout the investigation of exothermic reaction influence.

In the absence of exothermic reaction ($F_k = 0$), the heat source is represented by the two wavy vertical sides of the enclosure. The streams are driven by the buoyant force and the effect of the Ra value of 10^5 is dominant generating two vortices that have the same size but their locations are affected by the naturally generated current. The rise in F_k

from 0 to 4 not only results in extending the size of the vortex downward in the lower left section of the cavity but also causes the vortex size located in the top right section of the cavity to increase. The heat generated by the exothermic reaction intensifies the thermal gradients and causes the growth of vortices with augmenting F_k showing stronger buoyancy-driven circulation. Additionally, another two vortices, in the upper right wavy corner and the left wavy corner of the enclosure, started to appear when F_k rises to 1 and these vortices' size further increased when F_k increased. The existence of exothermic reaction contributes to diminishing the maximum velocity of nanofluid by 14.28% only, but it seems that the augmentation of F_k from 1 to 4 did not show any reduction in the nanofluid highest flow streams below 60. The influence of an exothermic reaction has a significant insight into heat transmission. Once an exothermic reaction is generated, more heat is added to the system leading to an intensification of heat in the top section of the cavity that is distributed anticlockwise where the hot streamlines extend toward the top surface of the circle and the left cold wall due to the flow circulation driven by the buoyancy strength. The trend of intensifying F_k number from 1 to 4, in the lower section of the cavity, can be noticed to have an extension in the heat towards the center of the whole enclosure. Increasing the F_k value to higher values greater than 2, results in enhancing the heat transfer in the cavity having the greater influence within the top section of the cavity owing to the flow circulation and the existence of the circular objects in the center of each section of the enclosure. The figures for the mean Nusselt number shown in Figure 8 reveal a significant rise as a result of augmenting the F_k values. It is discovered that Nu_{avg} increases noticeably when F_k is increased from 0 to 1, 2, 3, and 4, reaching increases of 16.42%, 34.33%, 52.24%, and 76.12%, respectively. When compared to the work done by N. Roy [12], a similar trend is noticed.

Figure 9 presents the results of hot wall wave number variation and their influences on heat transmission and nanofluid ($\varphi = 0.06$) stream velocity in the presence of a magnetic field (Ha=15) and keeping the other parameters at a fixed value (Ra=10^5 and F_k=1). The results show that doubling the hot wall wave results in a drop in maximum stream speed by 22.22% but streams return to speed up back again to the original value of 45 when using a single wave of both high-temperature walls. The vortices' size in case 2 (double waves) seems to be smaller when compared to the cases of having single or triple waves at the hot surfaces. Intensifying the number of waves causes the appearance of small vortices at the corners which become more noticeable as wavelengths number intensified. The trend of streamlines tends to show a clear enhancement of heat transmission in the top area that surrounds the circular objects. Adding more waves for the hot surfaces means augmenting the surface area of the heat source resulting in intensifying the heat transmitted within the cavity keeping the same surface area of the cold walls. This scheme translated the importance of increasing the dissipated heat with the wavelength amplification. However, it can be noticed in Figure 10 that the optimum condition for enhancing the heat transmission was reached when conducting the natural convection within the cavity of 2 waves (case 2) rather than having single or triple-waved active

12

walls cavity. As illustrated in Figure 11, increasing the wavelength of the cavity from a single wave to double waves achieved a rise in Nu_{avg} by 4.41%; however, further intensification of the active wavelength to 3 waves caused a slight drop in Nu_{avg} of this percent. This pattern may be explained physically by the fact that more waves increase the hot walls' surface area, which enhances heat dispersion within the cavity and amplifies the heat source. Excessive waves, on the other hand, create smaller vortices, which impede more widespread heat exchange by creating more confined circulation zones. Two waves thereby provide a balance, maximizing heat transmission and convective movement. The figures for the magnetic field inclination angles show an impressive influence on heat transmission as shown in Figure 11 which studies this impact for constant values of $Ra=10^5$, $Ha=25$, $F_k=1$, and $\phi=0.06$. It is proven that an inclined magnetic field of 75° has the highest impact on heat transfer, achieving a 6.94% increase in Nu_{avg} when compared to no rotational condition. When increasing the rotational angles of the magnetic field from 0 to 15, 30, 45, and 60 caused the Nu_{avg} to be enhanced by 1.48%, 3.3%, 4.95%, and 6.28% respectively. Reaching 90° magnetic field angle achieved better results but did not exceed the optimum status of 70°. Results also demonstrated the impact of the nanoparticles of ferric oxide-water nanofluid as illustrated by Nu_{avg} data given in Figure 12. It is found that when intensifying the nanoparticle volume fraction in the base fluid from 0 to 0.08, the mean Nusselt number is enhanced by achieving an increase in its value by 16.34%.

5. Conclusion

This work uses a magnetic field and an exothermic reaction to quantitatively investigate the rate of heat transfer of a ferric oxide-water nanofluid in a complicated wavy shape. Furthermore, the impact of incorporating two round items into the hollow was examined. A variety of important control elements were examined, including Ra (10^3, 10^4, and 10^5), Ha (0, 12, 25, and 60), F_k (0, 1, 2, 3, and 4), the inclination angle of the magnetic field (0, 15, 30, 45, 60, 75, and 90), wave amplitude (case 1=single wave, case 2= double wave, and case 3=triple waves), and the volume percentage of nanoparticles (0, 0.02, 0.04, 0.06, and 0.08). The results are shown in terms of isothermal contours, streamlines, and Nu_{avg} depending on the specified boundary conditions. The study addressed time dependent implications for a number of problem components. The research outcomes revealed the following impressive influences of the studied parameters on the natural convection within the staggered geometry:

- Comparatively, increasing Ra to 10^5 was shown to have the greatest influence on Nu_{avg}, rising by 142.85%, whilst increasing Ra to 10^4 resulted in a marginal increase in Nu_{avg} of about 20%.
- The maximum stream value was found to decrease as the Ha value increased. Also, it is demonstrated that reducing the Ha value from 60 to 0 results in a greater rise in the mean Nu.

- The maximum nanofluid velocity is only reduced by 14.28% due to the presence of an exothermic process. When F_k is increased from 0 to 1, 2, 3, and 4, it is found that Nu_{avg} grows considerably, reaching increases of 16.42%, 34.33%, 52.24%, and 76.12%, respectively for Ra=10^5, case 2 (wavelength=2), $\varphi = 0.04$, and Ha=0.

- The optimal circumstances for improving the rate of heat transfer are Ra=10^5, Φ =0.06, Ha=15, and F_k=1, which are achieved by conducting natural convection within the cavity with two waves (case 2) rather than single or triple-waved active walls.

- In the absence of a magnetic field, it is found that the best enhancement of N_{uavg} is achieved when intensifying the nanoparticle volume fraction in the base fluid from 0 to 0.08 for Ra=10^5 and F_k=1 reaching an increase of 16.34%.

6. Future work

The current work considers Fe₃O₄ with a range of Ra numbers. Some possible extensions for future work include:

• Considering a new nanofluid that could better enhance heat transfer.

• Exploring other applications, involving different geometries, to understand how the exothermic chemical reaction is influenced.

• Investigating new challenging parameters that could increase the novelty of the work.

References

[1]   Vijaybabu, T. R., "Influence of porous circular cylinder on MHD double-diffusive natural convection and entropy generation," *Int. J. Mech. Sci.*, vol. 206, no. May, p. 106625, (2021). https://doi: 10.1016/j.ijmecsci.2021.106625.

[2]   Alomari, M. A., Al-Farhany, K., Said, N. M., et al. "Numerical investigation of double-diffusive mixed convection in a split lid-driven curvilinear cavity," *Int. Commun. Heat Mass Transf.*, vol. 138, p. 106322, Nov. (2022). https:// doi: 10.1016/j.icheatmasstransfer.2022.106322.

[3]   Alomari, M. A., Al-Farhany, K., Al-Salami, Q. H., et al. "Magnetohydrodynamic mixed convection in lid-driven curvilinear enclosure with nanofluid and partial porous layer," *J. Magn. Magn. Mater.*, vol. 582, p. 170952, (2023). https:// doi: 10.1016/j.jmmm.2023.170952.

[4]   Al-Farhany, K., Alomari, M. A., Biswas, N. et al. "Magnetohydrodynamic double-diffusive mixed convection in a curvilinear cavity filled with nanofluid and containing conducting fins," *Int.*

Commun. Heat Mass Transf., vol. 144, p. 106802, (2023,)
https:// doi: 10.1016/j.icheatmasstransfer.2023.106802.

[5]   Kumar, T. P., Dharmaiah, G., Al-Farhany, K. et al., "Perturbation methodology for electromagnetic
        radiative fluxing of chemical reactive Casson fluid flow under heat source (sink) effectiveness,"
        Int. J. Mod. Phys. B, vol. 37, no. 28, p. 2350243, Feb. (2023).
        https:// doi: 10.1142/S0217979223502430.

[6]   Al-Chlaihawi, K. K., Alaydamee, H. H., Faisal, A. E. et al. "Newtonian and non-Newtonian
        nanofluids with entropy generation in conjugate natural convection of hybrid nanofluid-porous
        enclosures: A review," *Heat Transf.*, vol. 51, no. 2, pp. 1725–1745, Mar. (2022).
        https:// doi: 10.1002/htj.22372.

[7]   Alaydamee, H. H., Alomari, M. A., & Dawood, H. I. "Numerical modeling of free convection in a
        partially heated triangular enclosure with chamfer," *J. Phys. Conf. Ser.*, vol. 1973, no. 1, (2021).
        https:// doi: 10.1088/1742-6596/1973/1/012133.

[8]   Ahmed, H. E., Salman, B. H., & Kerbeet, A. S. "Heat transfer enhancement of turbulent
        forced nanofluid flow in a duct using triangular rib," *Int. J. Heat Mass Transf.*, vol. 134, pp. 30–
        40, (2019).
        https:// doi: 10.1016/j.ijheatmasstransfer.2018.12.163.

[9]   Assael, M. J., Antoniadis, K. D., Wakeham, W. A., et al. "Potential applications of nanofluids for
        heat transfer," *Int. J. Heat Mass Transf.*, vol. 138, pp. 597–607, (2019).
        https:// doi: 10.1016/j.ijheatmasstransfer.2019.04.086.

[10]   Hashimoto, S., Kurazono, K., & Yamauchi, T., "Anomalous enhancement of convective heat
        transfer with dispersed SiO2 particles in ethylene glycol/water nanofluid," *Int. J. Heat Mass
        Transf.*, vol. 150, p. 119302, (2020).
        https:// doi: 10.1016/j.ijheatmasstransfer.2019.119302.

[11]   Tehrani, B. M., & Rahbar-Kelishami, A. "Influence of enhanced mass transfer induced by
        Brownian motion on supported nanoliquids membrane: Experimental correlation and numerical
        modelling," *Int. J. Heat Mass Transf.*, vol. 148, p. 119034, (2020).
        https:// doi: 10.1016/j.ijheatmasstransfer.2019.119034.

[12]   Roy, N. C. "Natural convection in the annulus bounded by two wavy wall cylinders having a
        chemically reacting fluid," *Int. J. Heat Mass Transf.*, vol. 138, pp. 1082–1095, Aug. (2019).
        https:// doi: 10.1016/j.ijheatmasstransfer.2019.04.133.

[13]   Umadevi, R., Arivukkodi, D., Alhazmi, H., et al. "Heat transfer in a reversible esterification
        process of hydromagnetic Casson fluid with Arrhenius activation energy," *Case Stud. Therm.
        Eng.*, vol. 60, no. May, p. 104616, Aug. (2024).
        https:// doi: 10.1016/j.csite.2024.104616.

[14]   Hassan, A. M., Alomari, M. A., Al-Salami, Q. H., et al. "Numerical analysis of free convection
        under the influence of radiation and inclined MHD in a triangular cavity filled with hybrid
        nanofluid and a porous fin," *Int. J. Thermofluids*, vol. 24, p. 107993, Oct. (2024).
        https:// doi: 10.1016/j.ijft.2024.100843.

[15]   Minko, K. B., & Nashchekin, M. "Thermal performance of a metal hydride reactor for hydrogen
        storage with cooling/heating by natural convection," *Energy Storage Sav.*, vol. 2, no. 4, pp. 597–
        607, (2023).
        https:// doi: 10.1016/j.enss.2023.08.006.

[16]   Introini, C., Chiesa, D., Nastasi, M., et al. "A complete CFD study on natural convection in the
        TRIGA Mark II reactor," *Nucl. Eng. Des.*, vol. 403, p. 112118, (2023).
        https:// doi: 10.1016/j.nucengdes.2022.112118.

[17]   Freile, R., Tano, M., Balestra, P., et al. "Improved natural convection heat transfer correlations for
        reactor cavity cooling systems of high-temperature gas-cooled reactors: From computational fluid
        dynamics to Pronghorn," *Ann. Nucl. Energy*, vol. 163, p. 108547, (2021).
        https:// doi: 10.1016/j.anucene.2021.108547.

[18]   Campbell, A. N., Cardoso, S. S. S., & Hayhurst, A. N. "A comparison of measured temperatures

with those calculated numerically and analytically for an exothermic chemical reaction inside a spherical batch reactor with natural convection," *Chem. Eng. Sci.*, vol. 62, no. 11, pp. 3068–3082, (2007).
https:// doi: 10.1016/j.ces.2007.03.008.

[19]   Waqas, H., Khan, S. A., Yasmin, S., et al., "Galerkin finite element analysis for buoyancy driven copper-water nanofluid flow and heat transfer through fins enclosed inside a horizontal annulus: Applications to thermal engineering," *Case Stud. Therm. Eng.*, vol. 40, no. October, p. 102540, Dec. (2022).
https:// doi: 10.1016/j.csite.2022.102540.

[20]   Weppe, A., Moreau, F., & Saury, D. "Experimental investigation of a turbulent natural convection flow in a cubic cavity with an inner obstacle partially heated," *Int. J. Heat Mass Transf.*, vol. 194, p. 123052, (2022).
https:// doi: 10.1016/j.ijheatmasstransfer.2022.123052.

[21]   Izadi, S., Armaghani, T., Ghasemiasl, et al. "A comprehensive review on mixed convection of nanofluids in various shapes of enclosures," *Powder Technol.*, vol. 343, pp. 880–907, (2019).
https:// doi: 10.1016/j.powtec.2018.11.006.

[22]   Wang, L., Yang, X., Huang, C., et al. "Hybrid lattice Boltzmann-TVD simulation of natural convection of nanofluids in a partially heated square cavity using Buongiorno's model," *Appl. Therm. Eng.*, vol. 146, pp. 318–327, (2019).
 https:// doi: 10.1016/j.applthermaleng.2018.09.109.

[23]   Uddin, M. J., Rasel, S. K., Adewole, J. K., et al. "Finite element simulation on the convective double diffusive water-based copper oxide nanofluid flow in a square cavity having vertical wavy surfaces in presence of hydro-magnetic field," *Results Eng.*, vol. 13, no. February, p. 100364, (2022).
https:// doi: 10.1016/j.rineng.2022.100364.

[24]   Rashid, U., Lu, D., & Iqbal, Q. "Nanoparticles impacts on natural convection nanofluid flow and heat transfer inside a square cavity with fixed a circular obstacle," *Case Stud. Therm. Eng.*, vol. 44, no. December 2022, p. 102829, (2023).
https:// doi: 10.1016/j.csite.2023.102829.

[25]   Saha, T., Islam, T., Yeasmin, S., et al. "Thermal influence of heated fin on MHD natural convection flow of nanofluids inside a wavy square cavity," *Int. J. Thermofluids*, vol. 18, no. March, p. 100338, May (2023).
https:// doi: 10.1016/j.ijft.2023.100338.

[26]   Boukendil, M., El Moutaouakil, L., Zrikem, Z., et al. "Natural convection and surface radiation in an insulated square cavity with inner hot and cold square bodies," *Mater. Today Proc.*, vol. 45, no. xxxx, pp. 7282–7289, (2021).
https:// doi: 10.1016/j.matpr.2020.12.1011.

[27]   Panduro, E. A. C., Finotti, F., Largiller, G., et al. "A review of the use of nanofluids as heat-transfer fluids in parabolic-trough collectors," *Appl. Therm. Eng.*, vol. 211, no. November 2021, p. 118346, (2022).
https:// doi: 10.1016/j.applthermaleng.2022.118346.

[28]   Selimefendigil, F., & Öztop, H. F. "Thermal management and performance improvement by using coupled effects of magnetic field and phase change material for hybrid nanoliquid convection through a 3D vented cylindrical cavity," *Int. J. Heat Mass Transf.*, vol. 183, p. 122233, Feb. (2022).
https:// doi: 10.1016/j.ijheatmasstransfer.2021.122233.

[29]   Selimefendigil, F., & Öztop, H. F. "Thermal and phase change process in a branching T-channel under active magnetic field and two rotating inner cylinders: Analysis and predictions by radial basis neural networks," *Int. J. Heat Mass Transf.*, vol. 217, p. 124548, Dec. (2023).
https:// doi: 10.1016/j.ijheatmasstransfer.2023.124548.

[30]   Al-Amir, Q. R., Hamzah, H. K., Ali, F. H., et al., "Investigation of Natural Convection and

Entropy Generation in a Porous Titled Z-Staggered Cavity Saturated by TiO2-Water Nanofluid," *Int. J. Thermofluids*, vol. 19, no. June, p. 100395, (2023) https:// doi: 10.1016/j.ijft.2023.100395.

[31] Mansour, M. A., Siddiqa, S., Gorla, R. S. R., et al. "Effects of heat source and sink on entropy generation and MHD natural convection of Al2O3-Cu/water hybrid nanofluid filled with square porous cavity," *Therm. Sci. Eng. Prog.*, vol. 6, pp. 57–71, (2018). https:// doi: 10.1016/j.tsep.2017.10.014.

[32] Sheikholeslami, M., Li, Z., & Shamlooei, M. J. P. L. A. "Nanofluid MHD natural convection through a porous complex shaped cavity considering thermal radiation," *Phys. Lett. Sect. A Gen. At. Solid State Phys.*, vol. 382, no. 24, pp. 1615–1632, (2018). https:// doi: 10.1016/j.physleta.2018.04.006.

[33] Rashad, A. M., Armaghani, T., Chamkha, A. J., et al. "Entropy generation and MHD natural convection of a nanofluid in an inclined square porous cavity: Effects of a heat sink and source size and location," *Chinese J. Phys.*, vol. 56, no. 1, pp. 193–211, (2018). hiips:// doi: 10.1016/j.cjph.2017.11.026.

[34] Sajjadi, H., Delouei, A. A., Atashafrooz, M., et al. "Double MRT Lattice Boltzmann simulation of 3-D MHD natural convection in a cubic cavity with sinusoidal temperature distribution utilizing nanofluid," *Int. J. Heat Mass Transf.*, vol. 126, pp. 489–503, (2018) https:// doi: 10.1016/j.ijheatmasstransfer.2018.05.064.

[35] Kodi, R., Ganteda, C., Dasore, A., et al. "Influence of MHD mixed convection flow for maxwell nanofluid through a vertical cone with porous material in the existence of variable heat conductivity and diffusion," *Case Stud. Therm. Eng.*, vol. 44, no. January, p. 102875, (2023). https:// doi: 10.1016/j.csite.2023.102875.

[36] Mourad, A., Aissa, A., Abed, A. M., et al., "MHD natural convection of Fe3O4- MWCNT/Water hybrid nanofluid filled in a porous annulus between a circular cylinder and Koch snowflake," *Alexandria Eng. J.*, vol. 65, pp. 367–382, (2023). https:// doi: 10.1016/j.aej.2022.09.035.

[37] Tasnim, S., Mitra, A., Saha, H., et al. "MHD conjugate natural convection and entropy generation of a nanofluid filled square enclosure with multiple heat-generating elements in the presence of Joule heating," *Results Eng.*, vol. 17, no. January, p. 100993, (2023). https:// doi: 10.1016/j.rineng.2023.100993.

[38] Geridonmez, B. P., & Oztop, H. F. "MHD natural convection in a cavity in the presence of cross partial magnetic fields and Al2O3-water nanofluid," *Comput. Math. with Appl.*, vol. 80, no. 12, pp. 2796–2810, (2020). https:// doi: 10.1016/j.camwa.2020.10.003.

[39] Campbell, A. N., Cardoso, S. S. S., & Hayhurst, A. N. A., "A comparison of measured temperatures with those calculated numerically and analytically for an exothermic chemical reaction inside a spherical batch reactor with natural convection," *Chem. Eng. Sci.*, vol. 62, no. 11, pp. 3068–3082, (2007). https:// doi: 10.1016/j.ces.2007.03.008.

[40] Hussain, Z., Alshomrani, A. S., Muhammad, T., et al. "Entropy analysis in mixed convective flow of hybrid nanofluid subject to melting heat and chemical reactions," *Case Stud. Therm. Eng.*, vol. 34, p. 101972, (2022). https:// doi: 10.1016/j.csite.2022.101972.

[41] Reddy, P. S., Sreedevi, P., & Chamkha, A. J. "MHD boundary layer flow, heat and mass transfer analysis over a rotating disk through porous medium saturated by Cu-water and Ag-water nanofluid with chemical reaction," *Powder Technol.*, vol. 307, pp. 46–55, (2017). https:// doi: 10.1016/j.powtec.2016.11.017.

[42] Sreedevi, P., Reddy, P. S., & Chamkha, A. J. "Heat and mass transfer analysis of nanofluid over linear and non-linear stretching surfaces with thermal radiation and chemical reaction," *Powder Technol.*, vol. 315, pp. 194–204, (2017).

https:// doi: 10.1016/j.powtec.2017.03.059.

[43]   Hasan, M. M., Uddin, M. J., & Nasrin, R. "Exothermic chemical reaction of magneto-convective nanofluid flow in a square cavity," *Int. J. Thermofluids*, vol. 16, no. October, p. 100236, (2022) https// doi: 10.1016/j.ijft.2022.100236.

[44]   Arifuzzaman, M., & Uddin, M. J. "Convective flow of alumina–water nanofluid in a square vessel in presence of the exothermic chemical reaction and hydromagnetic field," *Results Eng.*, vol. 10, no. May, (2021).
https:// doi: 10.1016/j.rineng.2021.100226.

[45]   Rahman, M. M., Pop, I., & Saghir, M. Z. "Steady free convection flow within a titled nanofluid saturated porous cavity in the presence of a sloping magnetic field energized by an exothermic chemical reaction administered by Arrhenius kinetics," *Int. J. Heat Mass Transf.*, vol. 129, pp. 198–211, (2019).
https:// doi: 10.1016/j.ijheatmasstransfer.2018.09.105.

[46]   Yadav, D. "Impact of chemical reaction on the convective heat transport in nanofluid occupying in porous enclosures: A realistic approach," Int. J. Mech. Sci., vol. 157–158, no. January, pp. 357–373, (2019).
https:// doi: 10.1016/j.ijmecsci.2019.04.034.

[47]   Yadav, D., Awasthi, M. K., Ragoju, R., et al. "The impact of rotation on the onset of cellular convective movement in a casson fluid saturated permeable layer with temperature dependent thermal conductivity and viscosity deviations," *Chinese J. Phys.*, vol. 91, pp. 262–277, Oct. (2024).
https:// doi: 10.1016/j.cjph.2024.07.020.

[48]   Yadav, D., Awasthi, M. K., Ragoju, R., et al. "Impact of viscous dissipation, throughflow and rotation on the thermal convective instability of Jeffrey fluid in a porous medium layer," *Eur. J. Mech. - B/Fluids*, vol. 109, pp. 55–65, Jan. (2025).
https:// doi: 10.1016/j.euromechflu.2024.09.002.

[49]   Lazarovici, A., Volpert, V., & Merkin, J. H. "Steady states, oscillations and heat explosion in a combustion problem with convection," *Eur. J. Mech. B/Fluids*, vol. 24, no. 2, pp. 189–203, (2005).
https:// doi: 10.1016/j.euromechflu.2004.06.007.

[50]   Roy, N. C., Hossain, A., & Gorla, R. S. "Natural convective flow of a chemically reacting fluid in an annulus," *Heat Transf. Res.*, vol. 48, no. 4, pp. 1345–1369, Jun. (2019).
https:// doi: 10.1002/htj.21435.

[51]   Gibanov, N. S., Sheremet, M. A., Oztop, H. F., et al. "Effect of uniform inclined magnetic field on mixed convection in a lid-driven cavity having a horizontal porous layer saturated with a ferrofluid," *Int. J. Heat Mass Transf.*, vol. 114, pp. 1086–1097, Nov. (2017).
https:// doi: 10.1016/j.ijheatmasstransfer.2017.07.001.

[52]   Islam, T., & Nasrin, R. "Thermal operation by nanofluids with various aspects: a comprehensive numerical appraisal," *Waves in Random and Complex Media*, pp. 1–30, (2022).
https:// doi: 10.1080/17455030.2022.2117430.

[53]   Bruggeman, V. D. "Berechnung verschiedener physikalischer Konstanten von heterogenen Substanzen. I. Dielektrizitätskonstanten und Leitfähigkeiten der Mischkörper aus isotropen Substanzen," *Ann. Phys.*, vol. 416, no. 7, pp. 636–664, Jan. (1935).
https:// doi: 10.1002/andp.19354160705.

[54]   Hasan, M. M., Uddin, M. J., & Nasrin, R. "Exothermic chemical reaction of magneto-convective nanofluid flow in a square cavity," *Int. J. Thermofluids*, vol. 16, p. 100236, (2022).
https:// doi: 10.1016/j.ijft.2022.100236.

[55]   Alaydamee, H. H., Alomari, M. A., Al-Salami, Q. H., et al. "Numerical analysis of unsteady free convection of Al2O3 inside a tubular reactor under the influences of exothermic reaction, and inclined MHD as an application to chemical reactor," *Results Phys.*, vol. 65, p. 107993, Oct. (2024).

https:// doi: 10.1016/j.rinp.2024.107993.

[56] Alaydamee, H. H., Alomari, M. A., Al-Salami, Q. H., et al. "Numerical analysis of unsteady free convection under the combined influence of inclined magnetohydrodynamic and exothermic chemical reaction in an enclosure filled with nanofluid," *Int. J. Thermofluids*, vol. 23, p. 100704, Aug. (2024).
https:// doi: 10.1016/j.ijft.2024.100704.

Figure 1: Geometry of the present study (staggered wavy cavity)
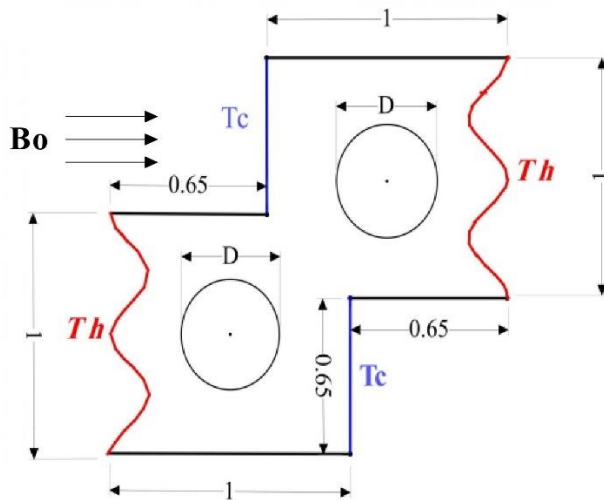
Figure 2: Validation of the present problem in terms of streamlines, and isothermal contours for $\phi = 0.05$, Ha = 40, $F_k = 2$, $\gamma = 0$, Ra=1e4 $T_0 = 25$ and τ=5 sec

Study	Isotherms	Streamlines
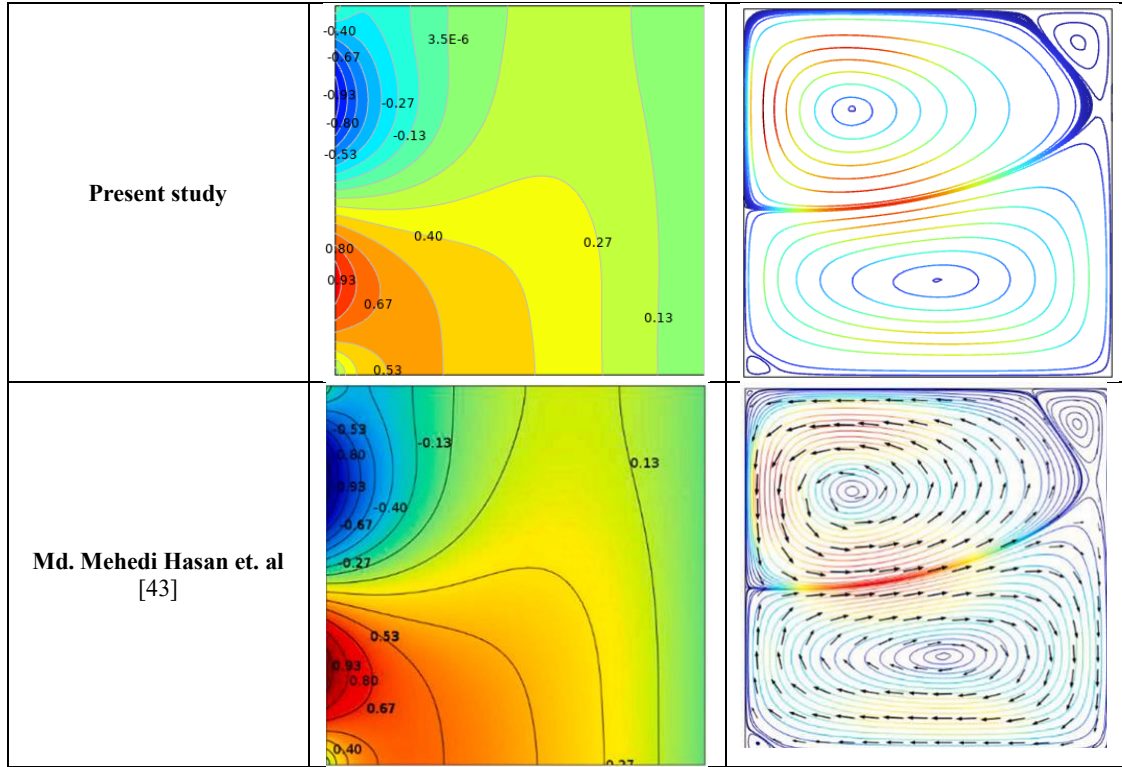
Table 1: *Thermophysical properties of ferric oxide-water nanofluid (Md. Mehedi Hasan et. al [43])*

Object	$\kappa[Wm^{-1}K^{-1}]$	$\mu[kgm^{-1}s^{-1}]$	$\beta[K^{-1}]$	$\rho[kgm^{-3}]$	$cp[Jkg^{-1}K^{-1}]$	$\sigma[Sm^{-1}]$
H_2O	0.613	0.001003	21×10^{-5}	997.1	4179	5.5×10^{-6}
Fe_3O_4	80.4		20.6×10^{-5}	5180	670	0.112×10^{-6}

Table 2: Mesh dependency for the present study at F_k=2, Ha=14, Ra=10^4, ϕ =0.03, Time=5 (21622 elements used)

No	No. elements	Mean Nu
1	2150	4.004
2	2498	4.105
3	3710	4.204
4	7802	4.419
5	**21622**	**4.577**
6	23898	4.579

Figure 3: Streamlines and Isotherms at Ha=12, case 2 (2 waves), $\phi = 0.02$, F_k=1, time=5 sec.

Ra	Streamline	Isotherm
Ra=10^3		
Ra=10^4		
Ra=10^5		
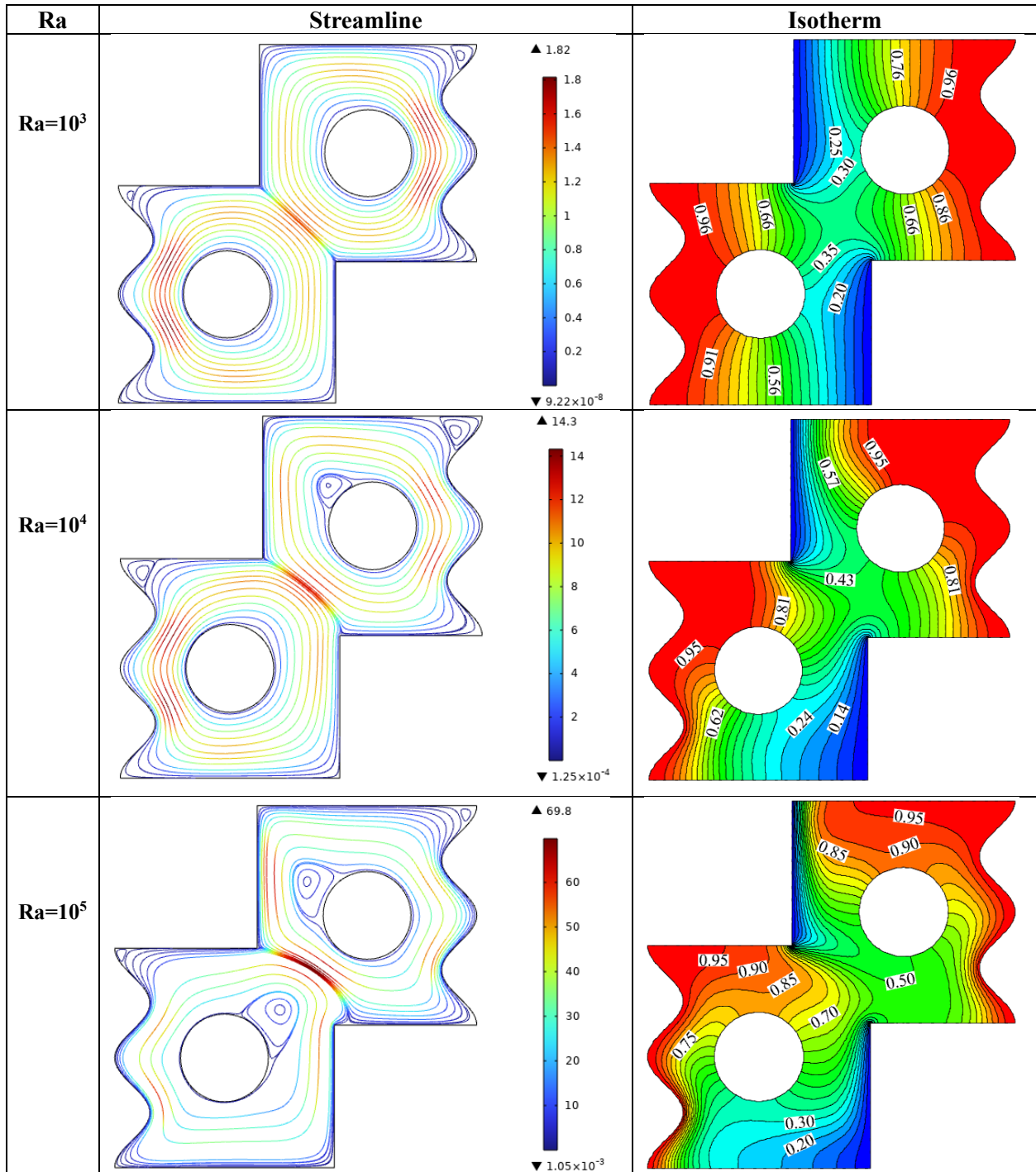
Figure 4: Average Nusselt number at Ha=12, case 2 (wavelength=2), $\phi = 0.02$, F_k=1
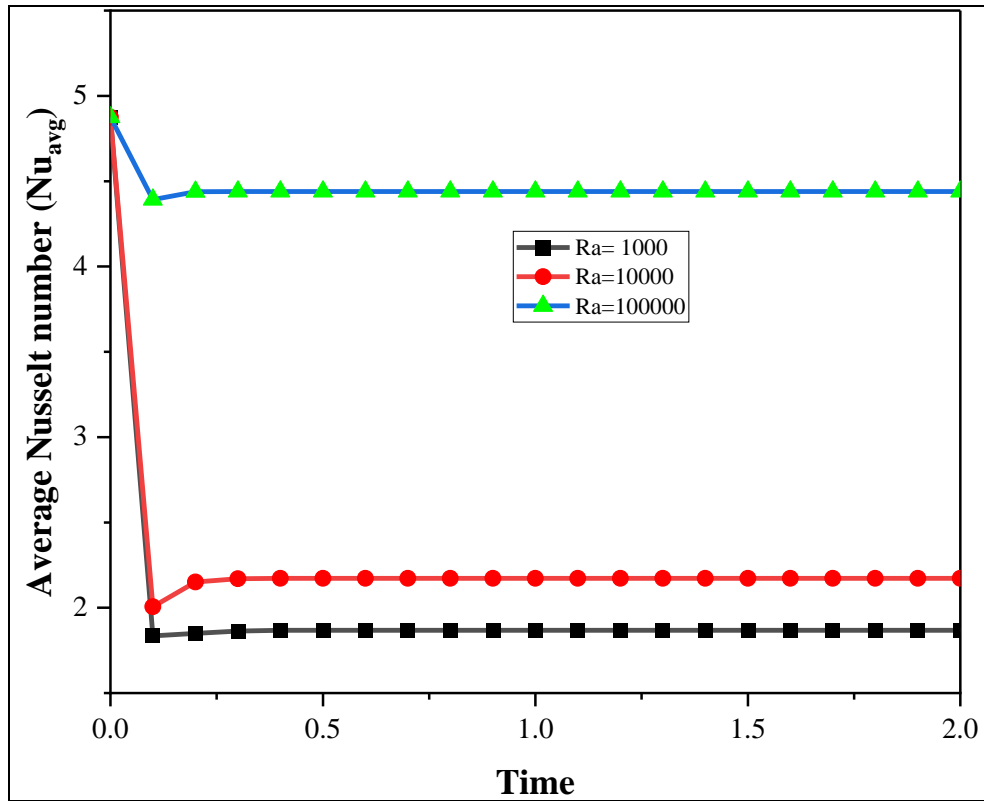
Figure 5: Streamlines and Isotherms for various Ha number at Ra=10^5, case 2 (wavelength=2), $\phi = 0.03$, F=1
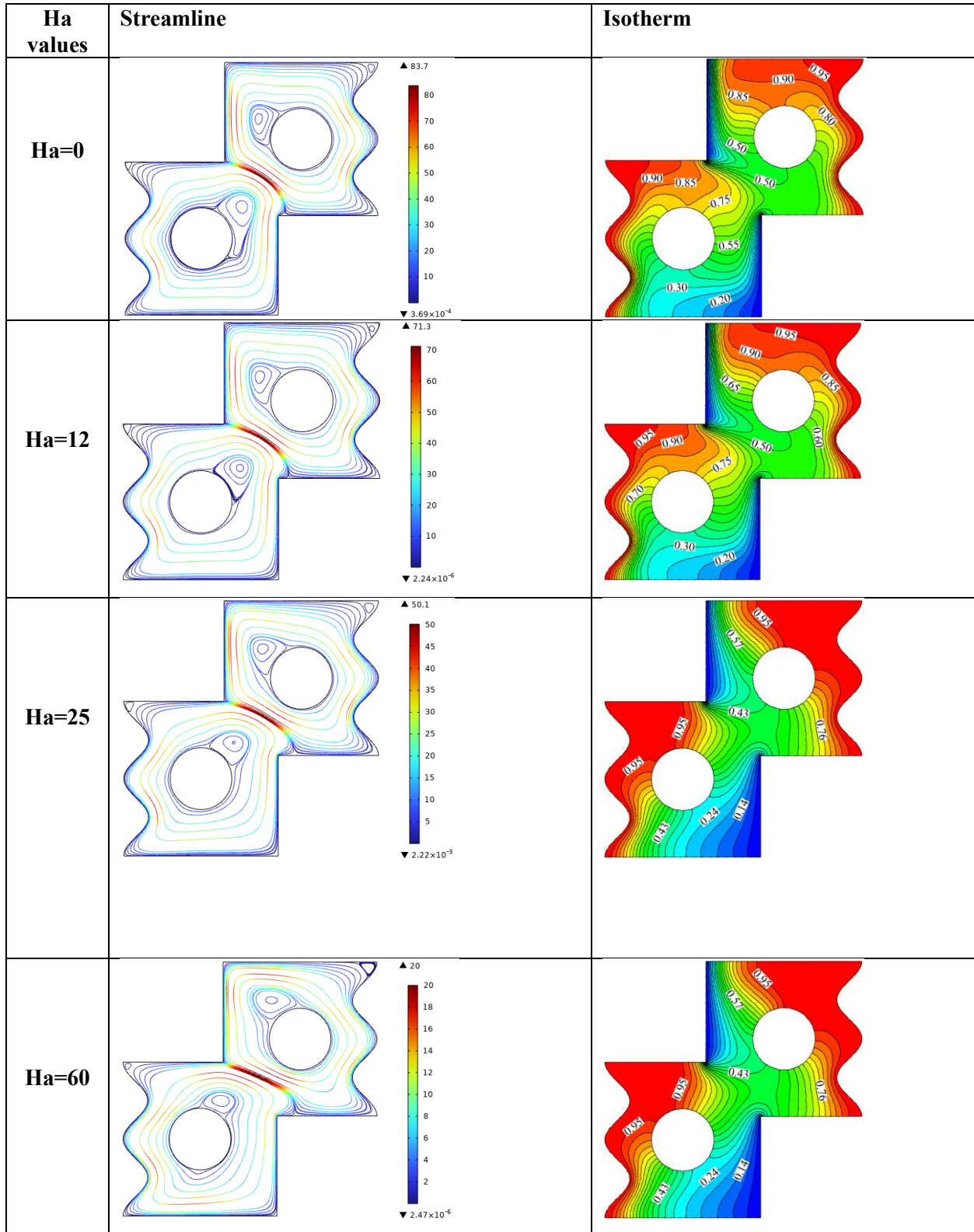
Ha values	Streamline	Isotherm
Ha=0		
Ha=12		
Ha=25		
Ha=60		

Figure 6: Average Nusselt number at Ra=10^5, case 2 (wavelength=3), $\phi = 0.03$, F_k=1
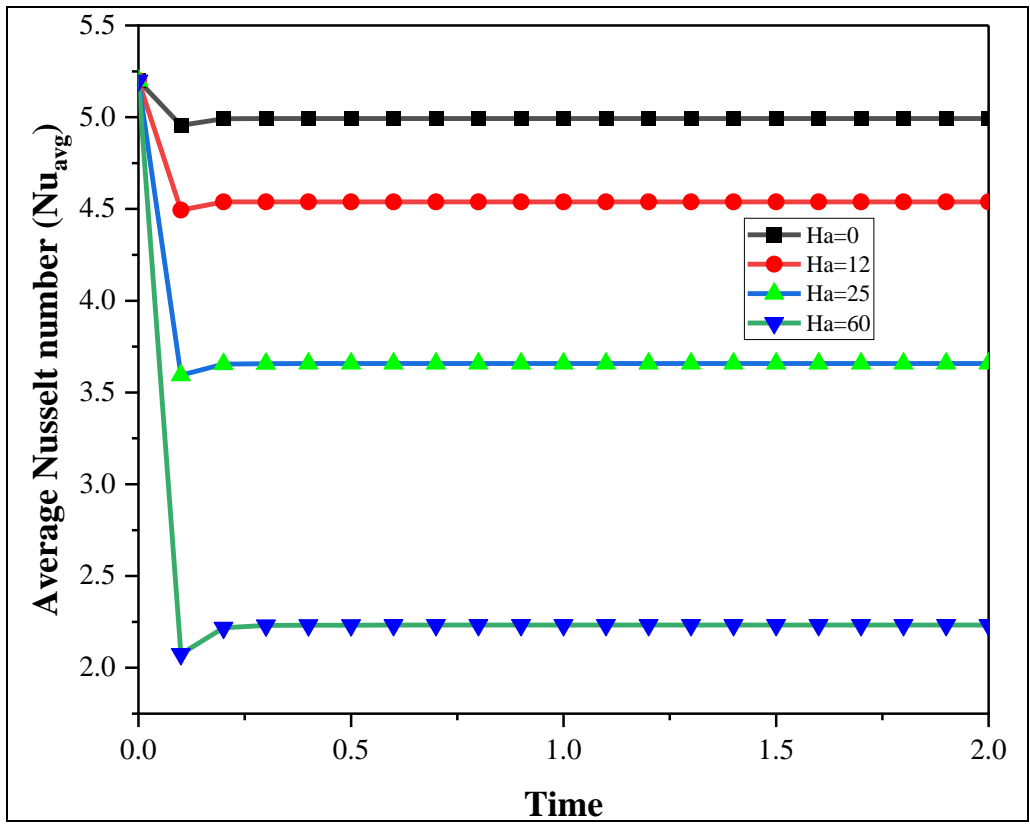
Figure 7: Streamlines and Isotherms at Ra=10^5, case 2 (wavelength=2), $\phi = 0.04$, Ha=0.

F_k number values	Streamline	Isotherm
$F_k=0$		
$F_k=1$		
$F_k=2$		
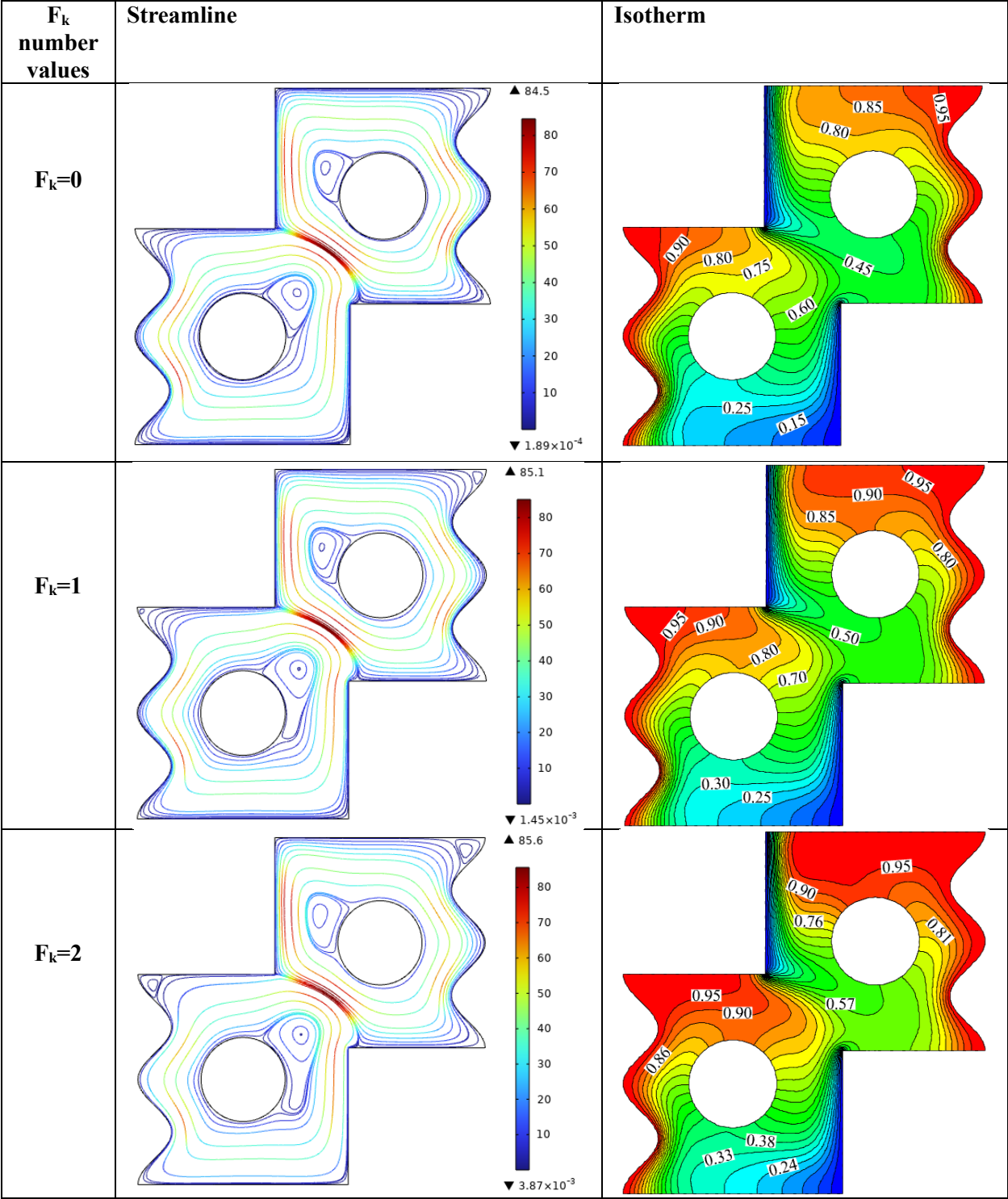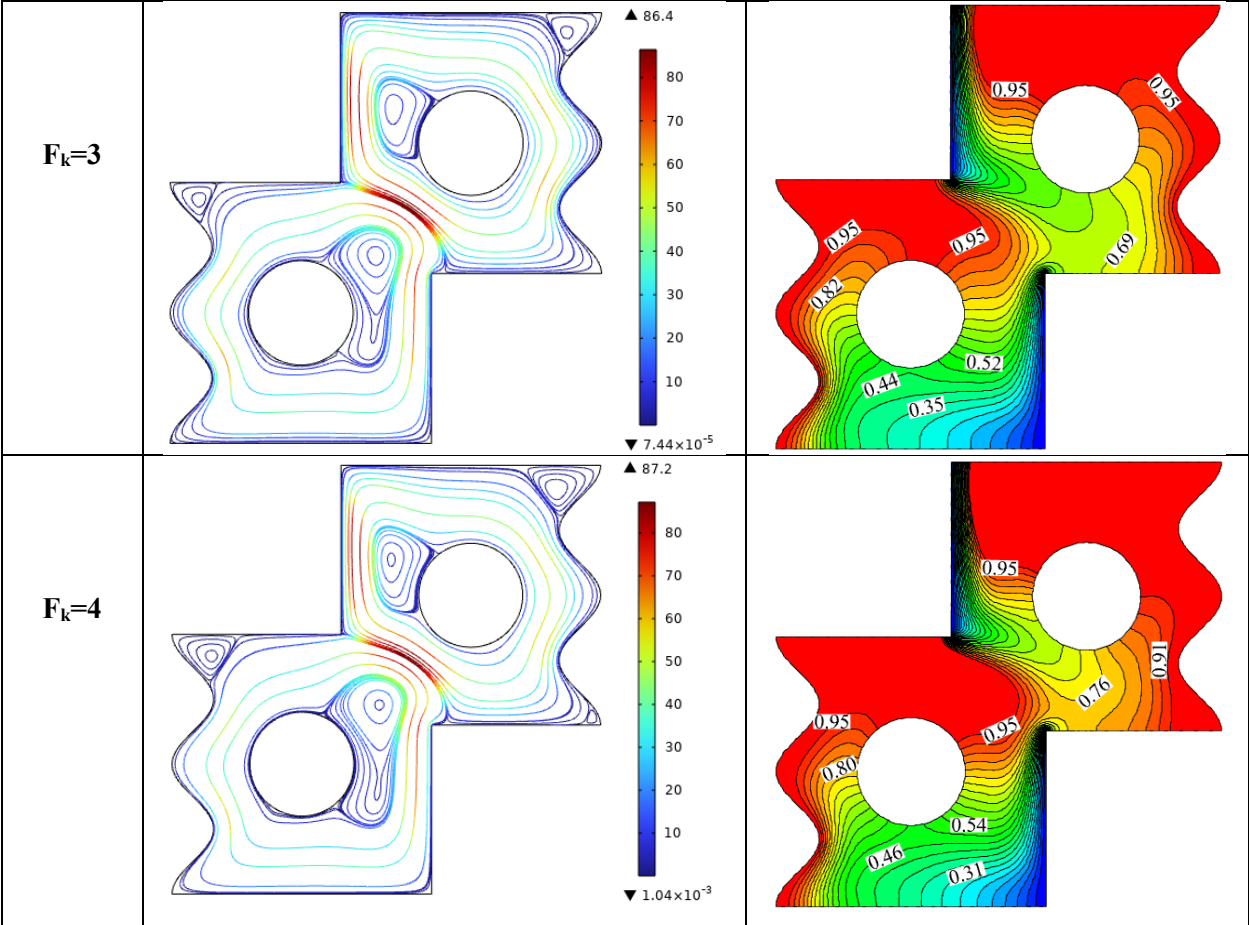
Figure 8: Average Nusselt number at Ra=10^5, case 2 (wavelength=3), $\phi = 0.04$, Ha=0.
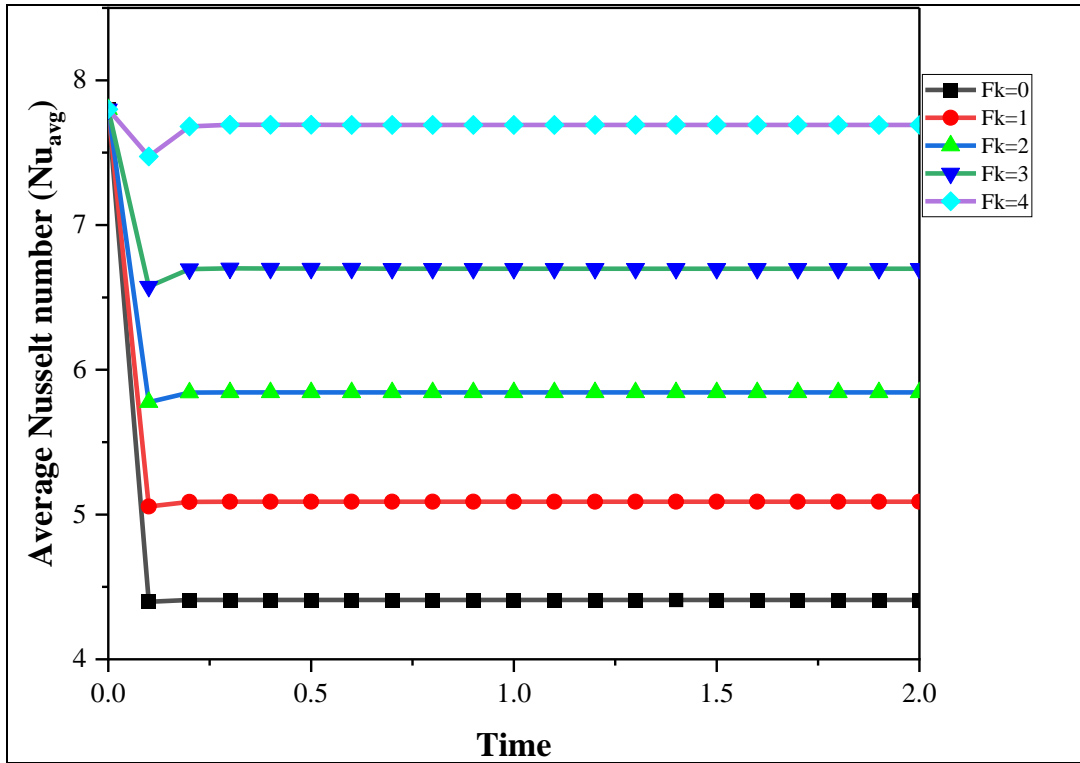
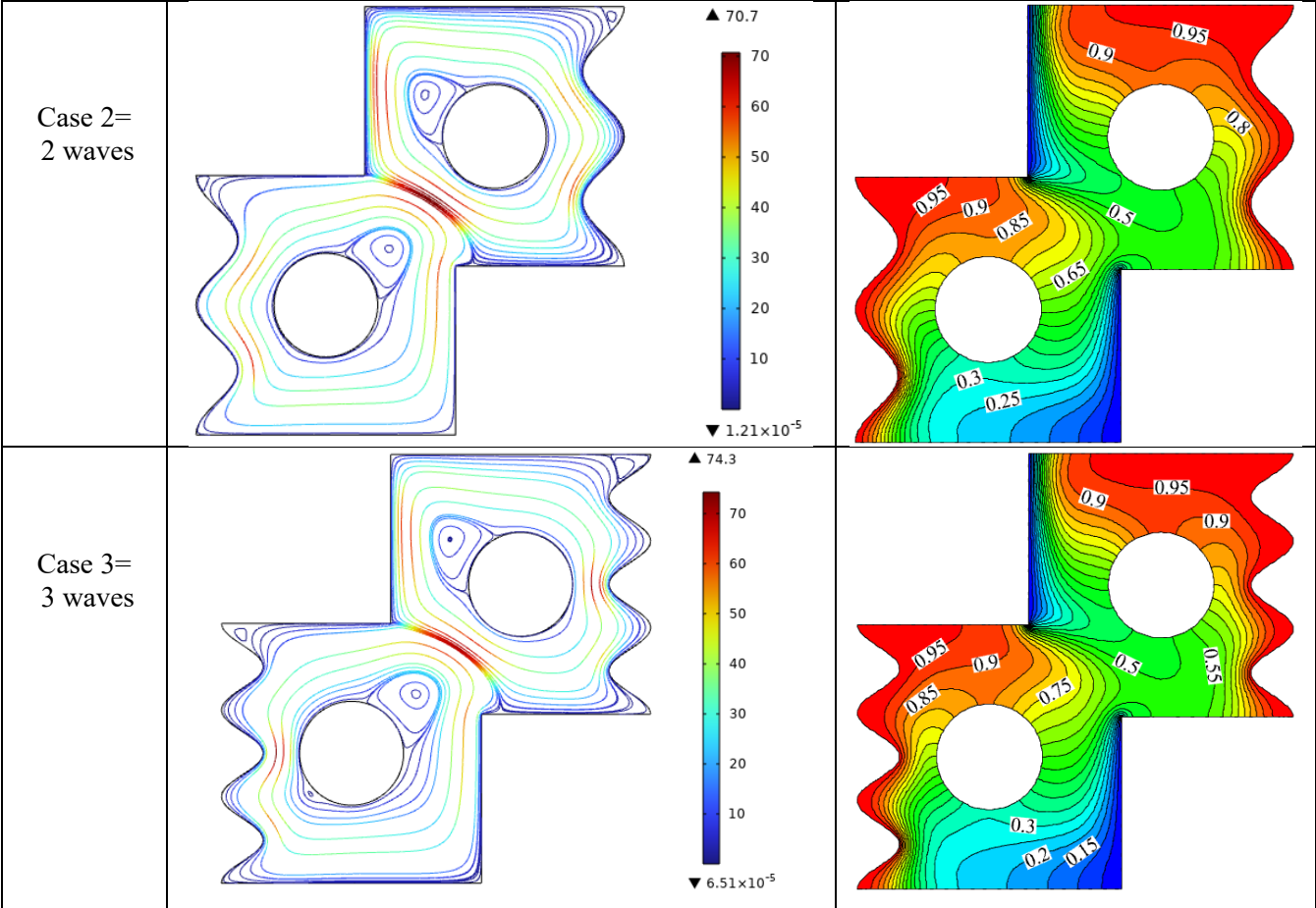**Figure 9:** Streamlines and Isotherms at Ra=10^5, $\phi = 0.06$, Ha=15, F_k=1

Wavelength cases	Streamline	Isotherm
Case 1= single wave		

Case 2= 2 waves		
Case 3= 3 waves		
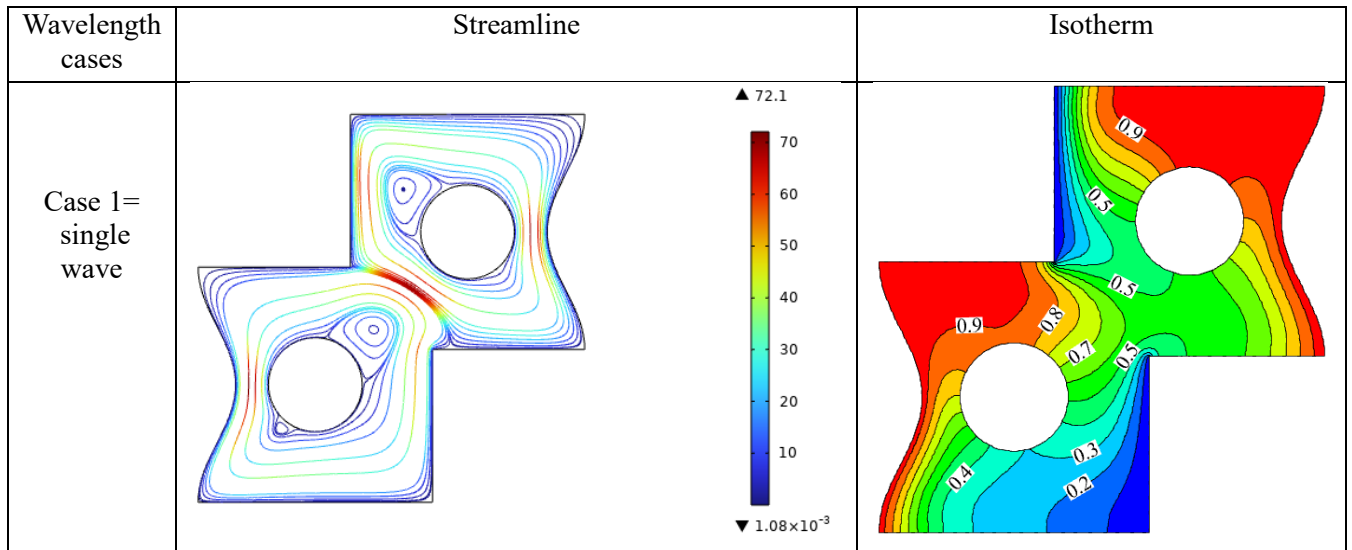
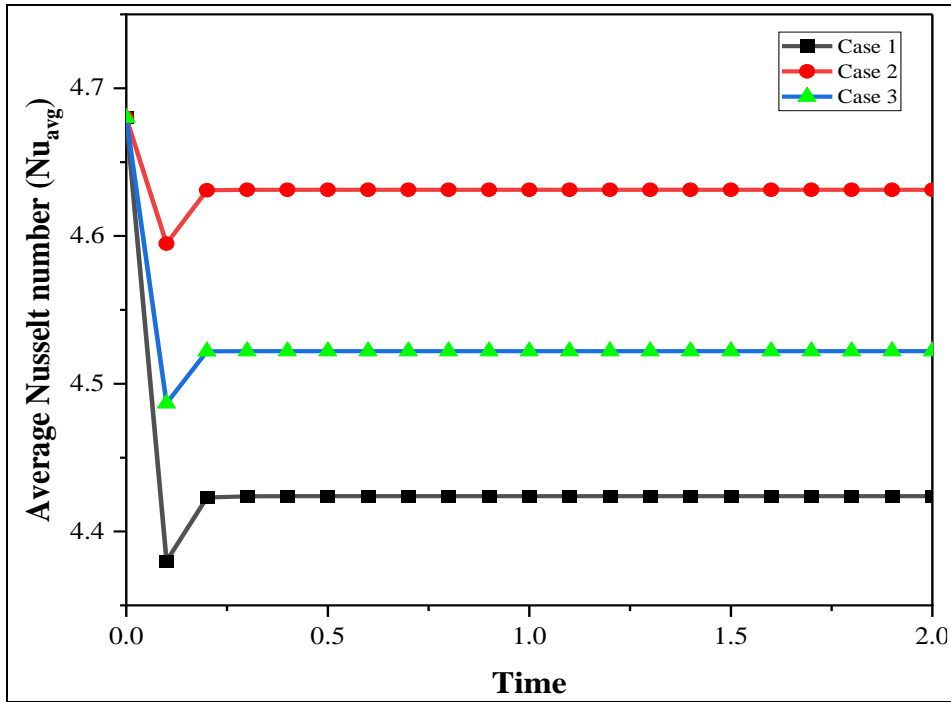**Figure 10:** Average Nusselt number at Ra=10^5, Ha=15, ϕ =0.06, F$_k$=1

Figure 11: Magnetic field Inclination influence on mean Nu number at Ra=10^5, Ha=25, F$_k$=1, Φ =0.06
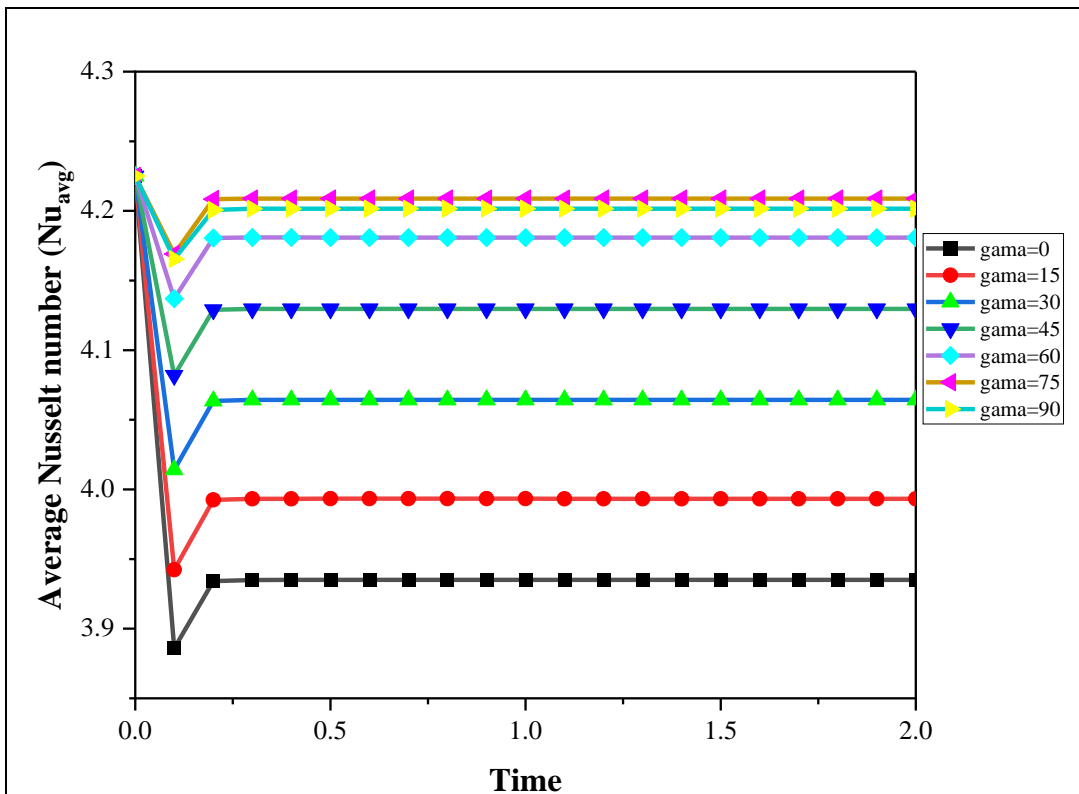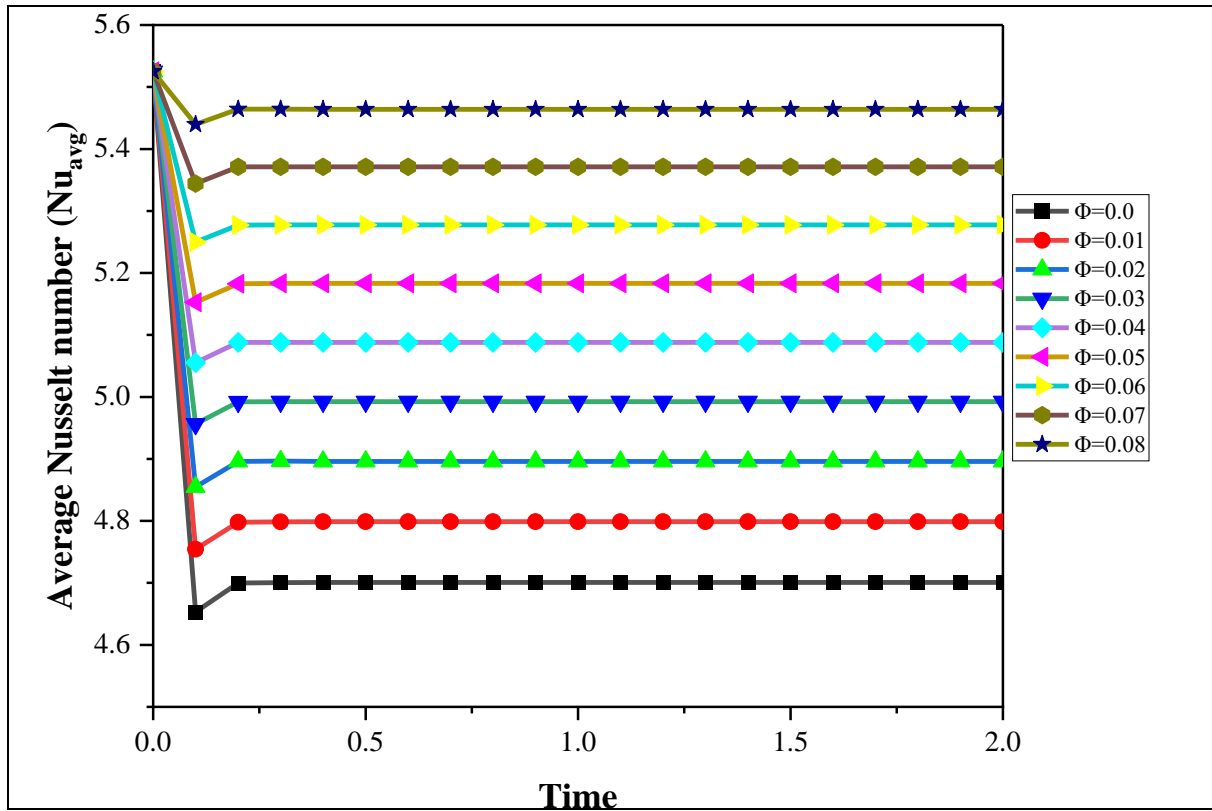
Figure 12: Fe_3O_4 nanoparticles impact on mean Nu number at Ra=10^5, Ha=25, F_k=1, ϕ =0.06, Ra=10^5, Ha=0, F_k=1

Farooq H. Ali is a Professor in the Mechanical Engineering Department at the College of Engineering, University of Babylon. He holds a B.Sc. and M.Sc. from the same institution. His academic contributions are underscored by the publication of numerous research papers in international journals, 46 in total, all indexed in the Scopus database, with an H-index of 12. Furthermore, he is currently pursuing a Ph.D. degree, focusing on absorption cooling processes utilizing solar energy.

Hussein H. Alaydamee is lecturer at the University of Al-Qadisiyah in chemical engineering. He is an expert in writing the academic paper with proper literature and an academic style.

Qusay H. Al-Salami is an Assistant Professor in Cihan university, he specialist in writing and revising an academic paper with a powerful ability to draw and optimize the results.

Hameed K. Hamza is a Professor in the Mechanical Engineering Department at the University of Babylon. His research areas are heat transfer, fluid flow, porous mediums, nanofluids, fluid-

structure interaction, and non-Newtonian fluids. His academic interests revolve around improving heat transfer, exploring solar energy applications, and delving into the potential of geothermal energy. Additionally, he has provided guidance and supervision to numerous MSc and PhD students.

Mohammed Azeez Alomari is a lecturer in the University of Al- Qadisiyah, he specialist in CFD of heat and mass transfer using different software's such as Ansys fluent, Star CCM and comsol multi physics.

Qusay Rasheed Al-amir is a Professor in the Mechanical Power Technical Engineering Department, College of Engineering and Technologies, Al-Mustaqbal University, Babylon, Iraq. He has made notable contributions to the field of air conditioning and refrigeration since 2010. His publications predominantly focus on subjects like heat and mass transfer, renewable energy, and solar energy.